



Energy-saving by low-power modes in ADSL2

Martin Wolkerstorfer^{a,*}, Driton Statovci^{a,1}, Tomas Nordström^{a,b,2}

^a FTW Telecommunications Research Center Vienna, Donau-City-Straße 1, A-1220 Vienna, Austria

^b Centre for Research on Embedded Systems (CERES), Halmstad University, Box 823, SE-30118 Halmstad, Sweden

ARTICLE INFO

Article history:

Available online 29 March 2012

Keywords:

Digital subscriber lines
Low-power modes
Optimization

ABSTRACT

The large number of broadband users and its forecast growth has recently triggered research on energy-efficiency in digital subscriber lines (DSLs). A promising technique are low-power modes (LPMs) as standardized in asymmetric DSL 2 (ADSL2) which let the DSL connection operate in downstream direction with reduced transmit rate and power. We study the problem of optimizing the LPM rate-level for energy-efficiency. A traffic-independent rate setting is proposed based on an analytical competitive framework. Also, a Markov chain based LPM model is derived which facilitates the fast numerical optimization of the LPM rate-level under realistic traffic models and system constraints. Simulation results under various traffic settings and DSL scenarios demonstrate energy savings by LPMs of around 30–40% of the ADSL2 transceiver's power consumption. Furthermore, they provide insights on how to set the LPM rate-levels in practice for energy-efficient DSL operation.

© 2012 Elsevier B.V. All rights reserved.

1. Introduction

Low-power modes (LPMs) are a standardized [1] technique in asymmetric digital subscriber lines 2 (ADSL2) aiming at reducing the power consumption at the central office (CO) side of the DSL link by reducing the downstream transmit rate and power. Our focus is on the optimization of the transmit rate in the LPM with respect to the expected average energy consumption. An optimization framework is proposed covering the case where one has no knowledge of the traffic arrivals, and the case where the distribution of arrival rates is known. In the latter case of known statistics we further distinguish between a worst-case analysis valid for any arrival distribution, and a more specific analysis based on a Markov chain model of the traffic and LPMs. This Markov chain model results in reduced simulation times which allows the exploration

of a larger set of simulation assumptions and scenarios. Furthermore, it assumes knowledge of a limited set of traffic statistics only, and captures LPM characteristics such as multiple LPM levels and time delays between power-mode changes.

1.1. Motivation and related work

The initial motivation for LPMs in DSL was the reduction of the heat dissipation and consequently cooling power needed at the CO [2] where typically a large number (up to thousands [3]) of DSL connections are terminated at the DSL access multiplexer (DSLAM). The LPM rate-level was supposed to be just high enough to keep up the basic DSL functionality (e.g., synchronization) and basic telephony services such as the voice-over-Internet protocol (VoIP). However, recently energy reduction itself has become an important design criterion in DSL [3,4], having impacts on system scalability (e.g., cooling requirements) and telco's operational expenditure (OPEX) and CO2 footprint. The European code of conduct on energy consumption of broadband equipment [4] even sets design goals for the energy consumption of DSL equipment. For example, a

* Corresponding author. Tel.: +43 1 5052830x27; fax: +43 1 505283099.

E-mail addresses: wolkerstorfer@ftw.at (M. Wolkerstorfer), statovci@ftw.at (D. Statovci), Nordstrom@hh.se (T. Nordström).

¹ Tel.: +43 1 5052830x44; fax: +43 1 505283099.

² Tel.: +46 0 35167334.

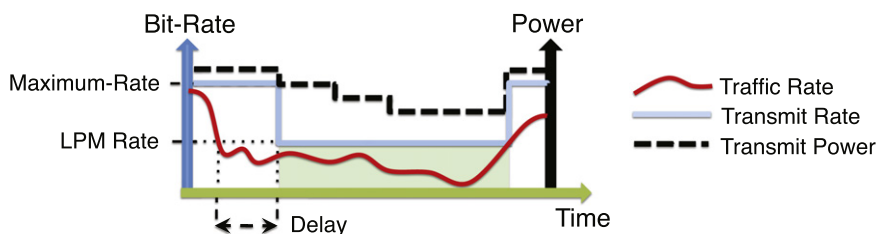


Fig. 1. Simplified illustration of the LPM functionality in ADSL2 [1].

power reduction by approximately 30% in the low-power state is foreseen for ADSL2 by 2014.³ The saved energy at the transceiver side results in an at least as high extra energy saving in the facility support equipment at the CO, a fact known as the “cascade effect” [5,6] or power usage effectiveness (PUE) [7]. Also, in [6] energy saving modes were found to be the most beneficial energy reduction strategy at the CO, a result based on the energy reduction targets in [4] and to a large extent in consequence of the cascading effect. This conclusion is further strengthened by the typically low usage of the DSL link. In [8] a network forecast of Telecom Italia for 2015–2020 is given. Therein the link usage (fraction of time the connection is used) and utilization (demanded data-rate compared to the maximum achievable rate) in the wired access network are quantified by 30% and 10%, respectively. In [9] private DSL and triple-play users are estimated to use the link less than 10% and 35%, respectively. Similarly, the study in [10] highlights that the time when the aggregate network traffic in North America is within 5% of the peak value over the day is only around 2 h, and in [11] the average Internet usage per day for Bavaria (Germany) was even reported to be as low as 37 min (2.6%). This indicates the potential for improving the energy efficiency in DSL by introducing LPMs and adaptive transmission rates. Summarizing, the efficiency of LPMs depends on the time operated in LPM and the transmit power spent in LPM. However, both the time spent in the LPM as well as the transmit power grow with increasing LPM rate, making the optimization of the LPM rate for energy-efficiency a non-trivial (e.g., non-convex) and, in general, traffic-dependent task.

Fig. 1 illustrates the functionality of LPMs in ADSL2 [1]. For example, one may define a delay between the time the traffic rate falls below the (single) LPM rate-level and the time the system enters the LPM state. Furthermore, the system exits the LPM instantaneously in order to avoid a user-perceived delay. The exit from the LPM state potentially causes instability in the network as it leads to changes in transmit power and hence in crosstalk noise received on other lines. We refer to [2,12–14] for studies showing the effects of LPMs on network stability and various solution approaches. The study in [14] is most related to our work, where buffer-state dependent policies were analyzed for switching between given power modes.

³ The precise targets foresee an energy reduction from 3.4 W in the full-power state to 2.4 W on the customer side and from 1.1 W to 0.7 W on the CO side.

Differently, in the present study we focus on the problem of selecting the rate at the LPM by analyzing the traffic-dependent energy savings.

Various proposals besides LPMs have been reported on how to save energy in DSL, for instance by the design of energy-efficient hardware modules [15–17], by the dimensioning and energy-efficient operation of the network processor [18], by wireless traffic aggregation at the user side and efficient line-card usage at the network side [19], by restricting the maximal margin and power cutback [20], or by the deployment of street cabinets [21–23]. The latter allows reducing the transmit power by shortening the cable length, and to reduce cooling requirements [24,25] by reducing the number of installed line cards. In [26] various techniques were used jointly to achieve a power reduction of around 30% in specific field trials. We refer to [3] for an overview on energy saving aspects in DSL.

1.2. An estimate of the achievable energy savings

The transceiver’s line-driver (LD) accounts for nearly 50% of the ADSL2 based DSLAM’s energy consumption [3]. Furthermore, the LD power consumption scales with the transmit power [15,27], where for ADSL2+ transceivers a maximal LD power reduction of 85% is possible by transmit power reduction [15]. This conforms to the predicted energy profile for DSLAMs in [8], showing an energy scaling potential of roughly 45% of the power consumption in full-power state. Differently, in [3] the energy savings by LPMs were more conservatively estimated at 20%. In [2] maximum savings of 420 mW were found in a specific experimental setup, which assuming a power consumption of an ADSL2 line-card of 1.2 W (the consumption target for 2011–2012 in [4]) corresponds to a saving of 28%. To obtain a concrete estimate of the energy saving potential of LPMs we assume a power consumption of an ADSL2 line-card of 1.2 W [4], an average saving in LD power consumption of 64%,⁴ a share of the LD-power in the line-card’s power budget of 50% [13], and a multiplicative energy-saving factor of 2 due to the PUE [3,5,6]. Altogether we obtain an energy saving potential of 6.7 kWh (or 0.67 Euro assuming an energy price of roughly 10 cent/kWh [28]) per year and DSL line.

⁴ This number is based on an average link usage of 20% and a potential LD power reduction in LPM during idle-times of 80% [15], resulting in an average saving potential of $(1 - 0.2) \times 0.8 = 0.64$.

1.3. Outline

We begin in Section 2 with an analysis of the rate-selection problem for LPMs in DSL. This parameter setting problem can be regarded as a degenerate online problem [29], which is concerned with making decisions under incomplete information on the future (e.g., traffic) requests and therefore the exact cost of the decisions. We will similarly analyze the LPM problem first from a competitive perspective, i.e., the traffic is considered to be optimized by an adversary. We refer to [30] and references therein for applications of competitive analysis in the design of dynamic power management policies. Alternatively, in Section 3 we develop a Markov model of the traffic on a session level allowing for a fast performance evaluation and optimization of LPMs. Note that in practice the LPM rate-level should be optimized based on the actual link usage statistics. Using the proposed model we demonstrate how traffic statistics can be integrated into LPM simulations, and exemplify the performance gain by optimizing the LPM rate-level by means of a specific set of such statistics. This model is then also extended to capture sequential LPMs and delay between LPM states. Differently to the energy saving estimate in Section 1.2 which is based on the average link usage, this approach provides estimates through a bottom-up modeling of the traffic and allows explicitly showing the impact of the optimization of LPM rate-levels and delay on the energy savings. Simulation results are provided in Section 4 under numerous rate-selection policies, system constraints, and DSL network scenarios. Our conclusions are summarized in Section 5.

2. Optimization models for low-power modes

We consider a single multi-carrier DSL transmission system and denote its transmission rate by ρ .⁵ We assume a monotonously increasing power cost function $c(\rho) > 0$ which maps the rate ρ , $0 \leq \rho \leq R$, to the power consumption of (parts of) the modem, where R is the maximum rate supported by the DSL system. As a practical example we use in our simulations the gap-approximation of the channel capacity in [31], additional noise [13] to account for the fluctuations in crosstalk noise caused by changing power modes on other lines connected through the same cable binder,⁶ and optimal greedy bit-loading [33] to compute the necessary transmit power for rate ρ , and further map the transmit power to the power consumption of the line-driver $c(\rho)$ through the model in [15].⁷ Furthermore, we abstract the (shaped) incoming traffic-rate by the marginal probability density function (pdf) $\pi(\rho)$, $0 \leq \rho \leq R$, where we initially do not assume any knowledge of $\pi(\rho)$. We restrict our atten-

⁵ Vectors, matrices and sets will be denoted by bold-faced lower/upper-case letters \mathbf{a} , \mathbf{A} , and \mathcal{A} , respectively, where $|A|$ represents the cardinality of a set and \mathbf{A}^T the transpose of a matrix. Specifically, the set \mathcal{R}_+ denotes the set of non-negative real numbers.

⁶ Other methods which have been proposed to cope with the variation in interference noise induced by LPMs are for instance a frequency-selective LPM and a slow LPM exit procedure [32].

⁷ The overall model satisfies the above assumption $c(\rho) > 0$ as line-drivers have a strictly positive “quiescent” power consumption at zero transmit power.

tion to systems which, beside the maximum rate R , support a finite number of L pre-defined low-power modes with corresponding rates $\mathbf{r} \in \mathcal{L} = \{\tilde{\mathbf{r}} \in \mathcal{R}^L | 0 \leq \tilde{r}_1 \leq \dots \leq \tilde{r}_L \leq R\}$. Assuming the system always transmits at a rate at least as high as the arrival rate, the expected total power under the LPM setting \mathbf{r} is given as

$$C^\pi(\mathbf{r}) = c(r_1) \int_0^{r_1} \pi(\rho) d\rho + c(r_2) \int_{r_1}^{r_2} \pi(\rho) d\rho + \dots + c(R) \int_{r_L}^R \pi(\rho) d\rho. \quad (1)$$

An obvious lower bound to the cost $C^\pi(\mathbf{r})$ of any LPM setting $\mathbf{r} \in \mathcal{L}$ is given by the minimal expected power

$$C^{*,\pi} = \int_0^R c(\rho) \pi(\rho) d\rho, \quad (2)$$

that is, the cost of an ideal system which continuously adapts its rate to the arrival rate.

2.1. Optimization under an unknown traffic arrival distribution

Intuitively we consider a LPM setting $\mathbf{r} \in \mathcal{L}$ a good choice if it results in a similar expected cost $C^\pi(\mathbf{r})$ to that of the ideal system $C^{*,\pi}$. Therefore we define our objective as the ratio of these two costs,⁸ leading to the *worst-case* LPM optimization problem given as

$$C^* = \underset{\mathbf{r} \in \mathcal{R}^L, 0 \leq r_1 \leq \dots \leq r_L \leq R}{\text{minimize}} \max_{\{\pi | \int_0^R \pi(\rho) d\rho = 1\}} \left\{ \frac{C^\pi(\mathbf{r})}{C^{*,\pi}} \right\}. \quad (3)$$

Note that in case we had solely considered $C^\pi(\mathbf{r})$ as our objective, the above question of the worst-case traffic would lead to the trivial solution $\pi(\rho) = 0$, for $0 \leq \rho < R$, and $\pi(R) = 1$, and an arbitrary LPM setting \mathbf{r} , which once more motivates the chosen ratio of costs in (3). Using the logarithmic cost function $c_{\text{dB}}(\rho) = 10 \log_{10}(c(\rho))$ the following result provides the analytical solution of the problem in (3).

Theorem 1. *Assuming $c(\cdot)$ is strictly positive and monotonously increasing, the optimum \mathbf{r}^* for the worst-case problem in (3) is given as*

$$r_l^* = c_{\text{dB}}^{-1} \left(\frac{1}{L+1} (c_{\text{dB}}(R) \cdot l + (L+1-l)c_{\text{dB}}(0)) \right), \quad 1 \leq l \leq L, \quad (4)$$

having the optimal objective

$$C^* = \sqrt[L+1]{\frac{c(R)}{c(0)}}. \quad (5)$$

See Appendix A for a proof.

Taking a practical example, using the ADSL2+ line-driver model in [15] we see that under a maximum

⁸ This ratio is a common objective in the online optimization literature [29] where it is referred to as “competitive ratio”.

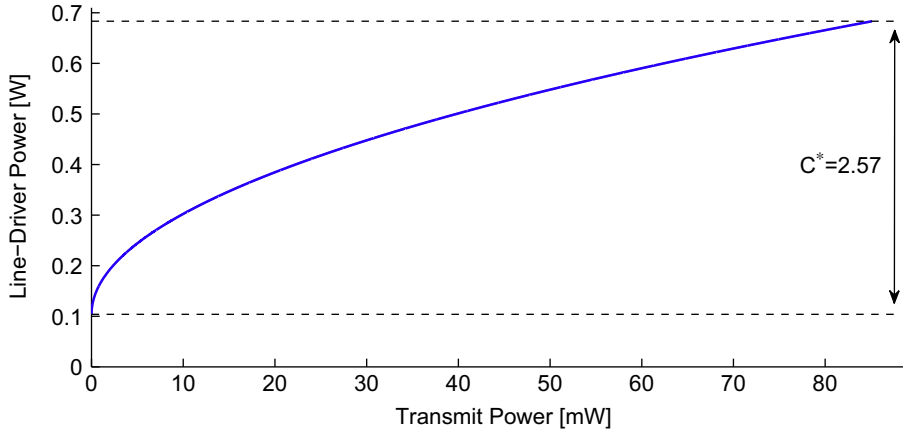


Fig. 2. ADSL2+ line-driver model [15] and its maximal cost ratio C^* .

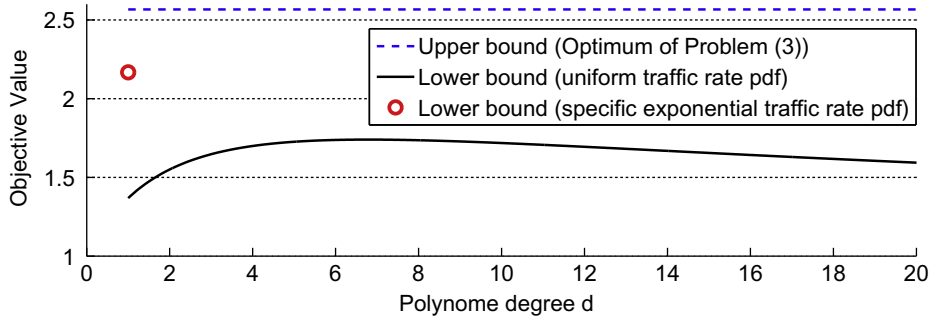


Fig. 3. Bounds on the optimal objective \tilde{C}^* of the problem in (6) for the polynomial cost functions in (7).

transmit power constraint of 19.3 dBm [34, Annex B] the cost ratio in (4) for a single LPM ($L = 1$) cannot exceed 2.57, cf. Fig. 2. In Section 4.2 we will show results on this cost ratio in a realistic traffic scenario. However, note that 2.57 will remain a valid upper-bound on the cost ratio in (3) for all optimized LPM settings in the rest of this work.

2.2. Optimization under a known traffic arrival distribution

Next let us assume that we have knowledge about the traffic distribution $\pi(\cdot)$ when we set the LPM rate levels \mathbf{r} . Intuitively, this should result in a cost somewhere between our worst-case analysis in Section 2.2 which was not based on any knowledge of the arrivals and their statistics, and the ideal system which follows the traffic rates in time. Knowledge of $\pi(\cdot)$ can be modeled by interchanging the two optimization operations in (3), resulting in the worst-case optimization problem under a *known* arrival distribution given as

$$\tilde{C}^* = \underset{\{\pi\}}{\text{maximize}} \underset{\mathbf{r} \in \mathcal{R}^L, 0 \leq r_1 \leq \dots \leq r_L \leq R}{\text{minimize}} \left\{ \frac{C^\pi(\mathbf{r})}{C^*, \pi} \right\}. \quad (6)$$

The objective in (6) characterizes the worst-case cost ratio for any possible arrival traffic characterized by its pdf $\pi(\cdot)$.

By duality arguments [35] it holds that $\tilde{C}^* \leq C^*$, i.e., the optimum in (3) upper bounds \tilde{C}^* , cf. Fig. 3. In order to derive lower bounds for \tilde{C}^* it suffices to pick any feasible pdf $\pi(\cdot)$. We demonstrate such lower bounds in Fig. 3 for single-level LPM ($L = 1$) under normalized polynomial cost functions of degree d ,⁹

$$\tilde{c}_{(d)}(\rho) = k\rho^d + c(0), \quad \text{where } k = \frac{c(R) - c(0)}{R^d}, \quad (7)$$

and uniform as well as exponential pdf $\pi^{\text{exp}}(\rho)$ and $\pi^{\text{uni}}(\rho)$, respectively, cf. Appendix B for a description of the computation of these bounds and the specific pdf settings. These bounds solely depend on $c(R)$ and $c(0)$ which are set based on the chosen ADSL2+ line-driver model [15] in Fig. 2 and a maximum transmit power of 19.3 dBm [34, Annex B]. Comparing the bounds under $\pi^{\text{exp}}(\rho)$ and $\pi^{\text{uni}}(\rho)$ for linear cost functions in Fig. 3 we find that the uniform distribution leads to a better LPM performance. The maximum value of the bound under a uniform pdf $\pi^{\text{uni}}(\rho)$ in Fig. 3 occurs for costs with a degree of approximately 6.8, while the limiting value for $d \rightarrow \infty$ is 1. Fitting the function in (7)

⁹ The given cost functions were chosen as they resemble the practical cost functions we use in simulations in Section 4. Furthermore, they are convex and therefore lend themselves for an analytical solution of the LPM rate-setting problem in (6).

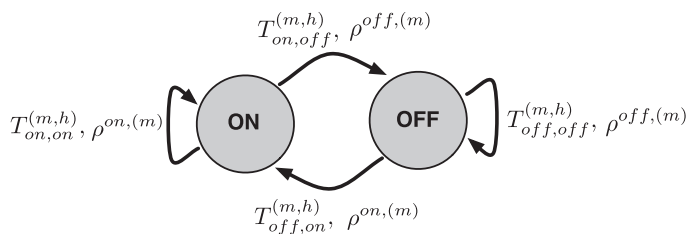


Fig. 4. On-off Markov model for a single application $m \in \mathcal{M}$ in hour h .

to the cost functions used in the simulations in Section 4 we find an average degree d in 1000 DSL scenarios of 2.4 (minimum 2.1 and maximum 2.8) with artificial noise and 3 (minimum 2.6 and maximum 3.2) without artificial noise, respectively, cf. Section 4 for details. In general the exact degree will depend on the considered noise and network scenario, the used line-driver model, etc.

Two important cases in practice, as we shall analyze by simulations in Section 4, are $L = 1$ and $L = 2$. While the above results assumed specific pdfs, the following structural result characterizes the two-level LPM solutions independently from the pdf $\pi(\cdot)$.

Theorem 2. *Assuming the optimal rate-level r^* under $L = 1$ (single-level LPM), and the optimal rate-levels $\tilde{r}^* \in \mathcal{R}_+^2$ under $L = 2$ (two-level LPM) for the problem in (6), we have that*

$$\tilde{r}_1^* \leq r^* \leq \tilde{r}_2^*. \quad (8)$$

See Appendix C for a proof.

Note that Theorem 2 offers a possibility for reducing the optimization complexity in the case of $L = 2$, as will become clearer in Section 3.1. We proceed in the following sections by analyzing the ratio $\frac{C^*(\mathbf{r})}{C^*(\mathbf{r}^*)}$ for more realistic traffic pdfs $\pi(\cdot)$.

3. Modeling low-power modes based on Markov chains

We derive a Markov model suitable for the fast performance evaluation of LPMs. We will begin in Section 3.1 by modeling each application as an on/off source and combining these sources in a joint Markov model of all traffic. Next we assign costs to subsets of the traffic arrival states according to the LPM definition to arrive at an LPM model in Section 3.2. Furthermore, in Section 3.3 we will show how this model can be extended to account for constraints encountered in practice.

3.1. Markovian traffic model

We model the arrival traffic on a session-level based on a finite set of M broadband applications indexed by $\mathcal{M} = \{1, \dots, M\}$, such as Internet protocol television (IPTV), video streaming, web, peer-to-peer (P2P) file sharing, interactive gaming, and voice-over-IP (VoIP). We denote by $s_m \in \{\text{on}, \text{off}\}$ the state of application $m \in \mathcal{M}$. When an application is in the on-state ($s_m = \text{on}$) it outputs a specific (aver-

age) data-rate $\rho^{\text{on}(m)}$ bps, while in the off-state ($s_m = \text{off}$) it delivers a data-rate $\rho^{\text{off}(m)} = 0$ bps. The set of all traffic states generated by the possible on-off combinations for the M applications is denoted by $\mathcal{S} = \{\mathbf{s} | s_m \in \{\text{on}, \text{off}\}, m \in \mathcal{M}\}$, where $|\mathcal{S}| = N = 2^M$. The arrival rate $\rho(\mathbf{s})$ in a specific state $\mathbf{s} \in \mathcal{S}$ is the sum of the rates per application $\rho^{s_m(m)}$ in the associated per-application states $s_m, m \in \mathcal{M}$, i.e.,

$$\rho(\mathbf{s}) = \sum_{m \in \mathcal{M}} \rho^{s_m(m)}. \quad (9)$$

We build a 2-state Markov model for each application m and hour $h \in \{1, \dots, 24\}$ with transitions occurring every second based on the transition matrix $\mathbf{T}^{(m,h)} \in \mathcal{R}_+^{2 \times 2}$, where, e.g., $T_{\text{on,off}}^{(m,h)}$ is the transition probability from the on-state to the off-state, cf. Fig. 4. The transition probabilities are obtained from application specific data on session characteristics given in [36,37] as follows: The average time in the (Markovian) on-state follows a geometric distribution with mean value $1/T_{\text{on,off}}^{(m,h)}$. Correspondingly we have

$$T_{\text{on,off}}^{(m,h)} = 1/t^{(m)}, \quad (10)$$

where $t^{(m)}$ is the average session duration¹⁰ in [s] of application m and $T_{\text{on,on}}^{(m,h)} = 1 - T_{\text{on,off}}^{(m,h)}$. Existence of a steady-state probability distribution for the Markov chain with transition matrix $\mathbf{T}^{(m,h)}$ follows from irreducibility [38] which holds for instance by assuming non-zero probabilities $T_{\text{on,on}}^{(m,h)}$, $T_{\text{on,off}}^{(m,h)}$, $T_{\text{off,on}}^{(m,h)}$, and $T_{\text{off,off}}^{(m,h)}$. Denoting the steady-state probability distribution of the Markov model of application m in hour h by $\mathbf{p}^{(m,h)} \in \mathcal{R}_+^2$ it holds that [38]

$$\mathbf{p}^{(m,h)} = (\mathbf{T}^{(m,h)})^T \mathbf{p}^{(m,h)}. \quad (11)$$

From (11) and $T_{\text{off,on}}^{(m,h)} + T_{\text{off,off}}^{(m,h)} = 1$ it follows that

$$p_2^{(m,h)} = T_{\text{on,off}}^{(m,h)} \left(T_{\text{off,on}}^{(m,h)} \right)^{-1} p_1^{(m,h)}. \quad (12)$$

The average fraction of time an application m is in the on-state in hour h is given by

$$p_1^{(m,h)} = S^{(h,m)} t^{(m)} (3600)^{-1}, \quad (13)$$

where $S^{(h,m)}$ is the average number of sessions in hour h for application m as obtained by the given number of sessions per day in [37, Table 3] (“residential broadband use case scenario”) and session probability distribution over the

¹⁰ The data are taken from [37, Table 1] where in case of an interval of session times we took the higher value and for P2P traffic we took the average session size and divide it by the average speed in the on-state, both given in [36].

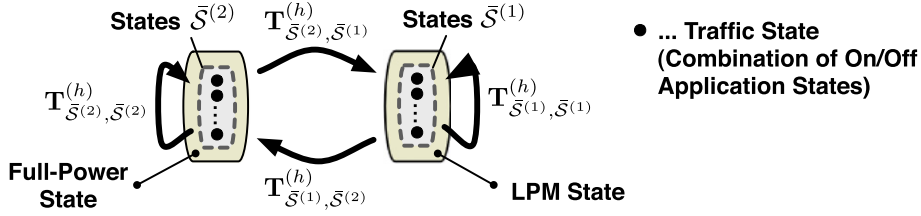


Fig. 5. Example of a Markov chain for one low-power mode in hour h .

day in [37, Figure 2].¹¹ Combining (10) with (12) and (13) and using $p_1^{(m,h)} + p_2^{(m,h)} = 1$ we obtain the transition probability

$$T_{\text{off,on}}^{(m,h)} = \frac{S^{(h,m)}}{3600 \left(1 - \frac{S^{(h,m)} \tau^{(m)}}{3600}\right)}, \quad (14)$$

and $T_{\text{off,off}}^{(m,h)} = 1 - T_{\text{off,on}}^{(m,h)}$. At this point we have fully defined all transition probabilities in the 2-state Markov model for application $m \in \mathcal{M}$ in hour h .

Under the assumption of independence among the state transitions of each application we have that the joint transition probability $T_{\mathbf{s}, \bar{\mathbf{s}}}^{(h)}$ from state \mathbf{s} to state $\bar{\mathbf{s}}$ can be computed as the product

$$T_{\mathbf{s}, \bar{\mathbf{s}}}^{(h)} = \prod_{m \in \mathcal{M}} T_{s_m, \bar{s}_m}^{(m,h)}. \quad (15)$$

The steady-state distribution of the joint Markovian traffic model with transition matrix $\mathbf{T}^{(h)} \in \mathcal{R}^{N \times N}$ constructed from transition probabilities $T_{\mathbf{s}, \bar{\mathbf{s}}}^{(h)}$, $\mathbf{s}, \bar{\mathbf{s}} \in \mathcal{S}$, is given by $\mathbf{p}^{(h)} \in \mathcal{R}_+^N$, where as above it holds that

$$\mathbf{p}^{(h)} = (\mathbf{T}^{(h)})^T \mathbf{p}^{(h)}. \quad (16)$$

Based on recent traffic models [36,37] we find that the most likely state in practice is the one where all applications are in the off-state. Therefore a low-complexity method to compute the distribution $\mathbf{p}^{(h)}$ in (16) is obtained through iterative multiplication with the transition matrix [39] beginning with the distribution vector $\tilde{\mathbf{p}}^{(h)}$ which is 1 in the all-off state and zero otherwise. Note that our model could benefit from information on the correlation of state transitions. Such information is currently only implicitly considered through the given changes in the session probability over the day and therefore in the state transition probabilities for each application.

3.2. LPM Markov chain

We proceed by extending this Markov chain of the traffic to model LPMs. For that purpose we partition the set of states \mathcal{S} into *exclusive* subsets $\bar{\mathcal{S}}^{(i)}$, $1 \leq i \leq L+1$, where

$$\bar{\mathcal{S}}^{(i)} = \begin{cases} \{\mathbf{s} \in \mathcal{S} | 0 \leq \rho(\mathbf{s}) \leq r_1\}, & \text{if } i = 1, \\ \{\mathbf{s} \in \mathcal{S} | r_{i-1} < \rho(\mathbf{s}) \leq r_i\}, & \text{if } 1 < i \leq L, \\ \{\mathbf{s} \in \mathcal{S} | r_L < \rho(\mathbf{s}) \leq R\}, & \text{if } i = L+1, \end{cases} \quad (17)$$

¹¹ Note that the chosen data leads to a transition matrix $\mathbf{T}^{(m,h)}$ with strictly positive entries and therefore to an irreducible chain with unique steady-state distribution [38].

and write $\mathbf{T}_{\bar{\mathcal{S}}^{(i)}, \bar{\mathcal{S}}^{(j)}}^{(h)} \in \mathcal{R}^{|\bar{\mathcal{S}}^{(i)}| \times |\bar{\mathcal{S}}^{(j)}|}$ to denote the partial transition matrix from all states $\mathbf{s} \in \bar{\mathcal{S}}^{(i)}$ to all states $\mathbf{s} \in \bar{\mathcal{S}}^{(j)}$. Equivalently, state transitions from power mode i into power mode j occur according to transition probabilities $\mathbf{T}_{\bar{\mathcal{S}}^{(i)}, \bar{\mathcal{S}}^{(j)}}^{(h)}$, cf. Fig. 5 which exemplarily depicts our LPM Markov model for a single LPM state ($L = 1$). Denoting by $p^{(h)}(\mathbf{s})$ the element of $\mathbf{p}^{(h)}$ associated with the joint traffic state $\mathbf{s} \in \mathcal{S}$ we can write the cost associated in hour h with an LPM setting \mathbf{r} similarly as in (1) as

$$C_h^\pi(\mathbf{r}) = c(R) \sum_{\mathbf{s} \in \bar{\mathcal{S}}^{(L+1)}} p^{(h)}(\mathbf{s}) + \sum_{\{l | 1 \leq l \leq L\}} c(r_l) \sum_{\mathbf{s} \in \bar{\mathcal{S}}^{(l)}} p^{(h)}(\mathbf{s}). \quad (18)$$

As the cost $c(\cdot)$ is monotonously increasing we can restrict our search for an optimal LPM setting \mathbf{r} to the set of arrival rates $\{\rho(\mathbf{s}) | \mathbf{s} \in \mathcal{S}\}$. Similarly as in (2), the cost of our ideal system which continuously follows the arrival rates is given by

$$C_h^{*,\pi} = \sum_{\mathbf{s} \in \mathcal{S}} c(\rho(\mathbf{s})) p^{(h)}(\mathbf{s}). \quad (19)$$

The total average cost can now be obtained by averaging the costs in (18) and (19) over all hours $h \in \{1, \dots, 24\}$, respectively. Note that with an increasing number of traffic states N Theorem 2 offers an opportunity for a less complex search for the optimum \mathbf{r} in case of $L=2$ by first (exhaustively) searching the optimum rate-level r^* under $L=1$ and then searching the two-level LPM rates in a restricted search space. More precisely, instead of evaluating the objective of all $N(N-1)/2$ combinations for r_1 and r_2 , we exhaustively search the value of the lower LPM rate r_1 in the restricted interval $[0, r^*]$ and test the objective values for all combinations with the higher LPM rate r_2 in the restricted interval $[r^*, R]$.

3.3. Delayed and sequential low-power modes (LPMs)

For reasons of network instability due to crosstalk among the copper lines deployed in the same cable bundle two timing constraints for LPMs have been introduced in the ADSL2 standard [1]: (a) a minimum time between the exit from and following entrance in the LPM and (b) a minimum time before the first power-trim in the LPM and between consecutive power trims, cf. the successive transmit power reduction indicated in Fig. 1. Both can take integer values between 0 and 255 s, cf. [2] for recommended settings. We therefore make the practical assumption that LPMs can only be changed to the next lower LPM (e.g., from LPM l to LPM $l-1$) after a certain delay, while the full-power mode can be activated instantaneously in

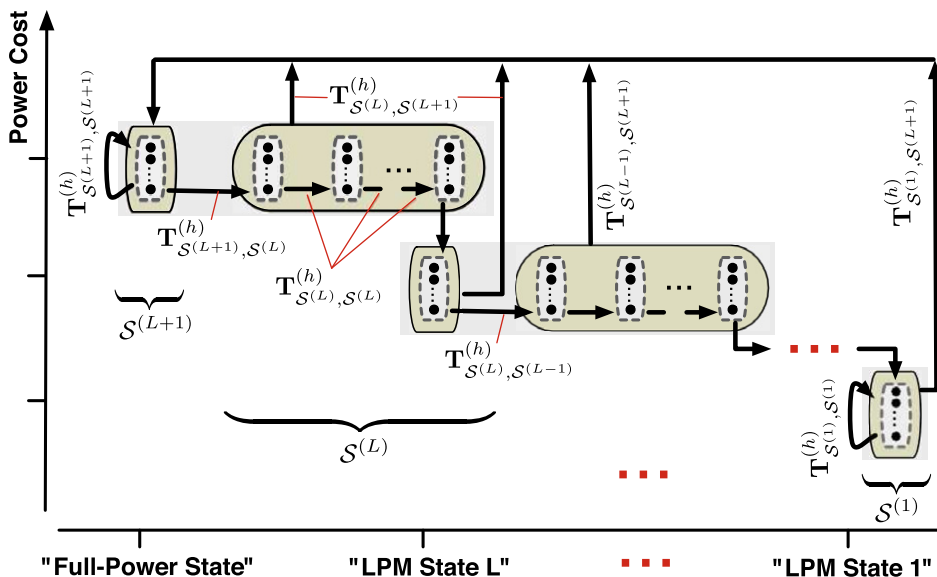


Fig. 6. Transition probabilities of a Markov chain for sequential low-power modes with delay.

order to avoid quality of service (QoS) degradation. The LPM model of Section 3.2 can be extended in a straightforward way to capture these requirements as schematically depicted in Fig. 6. Therein we partition the set of states \mathcal{S} into *non-exclusive* subsets $\mathcal{S}^{(i)}$, $1 \leq i \leq L+1$, where

$$\mathcal{S}^{(i)} = \begin{cases} \{\mathbf{s} \in \mathcal{S} | 0 \leq \rho(\mathbf{s}) \leq r_i\}, & \text{if } 1 \leq i \leq L, \\ \{\mathbf{s} \in \mathcal{S} | r_L < \rho(\mathbf{s}) \leq R\}, & \text{if } i = L+1, \end{cases} \quad (20)$$

and write $\mathbf{T}_{S^{(i)}, S^{(j)}}^{(h)}$ to denote the partial transition matrix from all states $\mathbf{s} \in \mathcal{S}^{(i)}$ to all states $\mathbf{s} \in \mathcal{S}^{(j)}$. Furthermore, $(D+1)$ denotes the number of seconds the arrival rate has to be below the LPM rate in order to go into the corresponding LPM. Note that the full Markov model has now $O(N \cdot L \cdot D + N \cdot L + N)$ states for the waiting periods, the LPMs and the full-power mode, respectively. The average cost is now computed similarly as in (18) with the waiting states having an associated cost of the next higher LPM or full-power mode, respectively. Note that multiple power trim procedures [1] can be modeled in a similar fashion with multiple delay queues per LPM and different associated costs. A possibly specified minimum time between an LPM exit and re-entrance [1] or a slow wake-up from any LPM to the full power state [32] can be modeled by a state queue with transitions $\mathbf{T}^{(h)}$ and appropriately assigned costs per state, similarly as in Fig. 6. In such a queue one moves from one state to the next at every time instance, thereby modeling a fixed (i.e., traffic-independent) time delay.

4. Performance evaluation

We evaluate the performance of LPMs with one or two rate-levels and with or without waiting delay before entering an LPM by simulation of an ADSL2+ system.

4.1. Simulation parameters

We uniformly sample 1000 network topologies with loop-lengths between 500 m and 3000 m, considering downstream transmission, British Telecom cables of type “BT-dwug” with 0.5 mm diameter [40], artificial noise (AN) calculated as the interference from 49 collocated disturbers added to a background noise of -120 dBm/Hz, the bandplan defined in [34, Annex B] with non-overlapped spectrum operation over the Integrated Services Digital Network (ISDN), a signal-to-noise ratio (SNR) gap Γ [31] of 12.8 dB (consisting of 9.8 dB modulation gap, 6 dB SNR margin, and 3 dB coding gain), and a maximum sum-power of 19.3 dBm. The traffic model is as described in Section 3 based on the session characteristics in [36,37] with $M=7$ selected services.¹² This results in $N=128$ traffic states and an equal number of possible arrival rates, out of which we can select the LPM rate-levels $\mathbf{r} \in \mathcal{R}_+^L$, cf. Section 3.2. This traffic model results in an average link usage (fraction of time the DSL link is used) over the day of 16.8% and an average (over scenarios and time) link utilization (fraction of the maximum achievable rate demanded by the user when the link is used) of 14.7%. Confidence intervals are given according to a Student’s t -test with a confidence level of 99%.

4.2. Average single-level LPM performance

We compare the single-level LPM under various rate setting policies to the continuously rate-adaptive system which upper-bounds the performance of LPMs, i.e., under any rate-setting \mathbf{r} and number of LPMs L .

¹² More precisely, the selected services are: Web, 2 IPTV services, VoIP, gaming, file-sharing, and video streaming with average on-state rates $\rho^{on(m)}$, $1 \leq m \leq M$, of 3.467 kbps, 3.415 Mbps, 80 kbps, 17 kbps, 792.2 bps, and 340 kbps, an average number of sessions per day of 2.5, 1, 2, 1, 0.14, and 1, and an average session duration $t^{(m)}$ of 0.083, 1, 0.058, 1, 0.576, and 1 h, respectively.

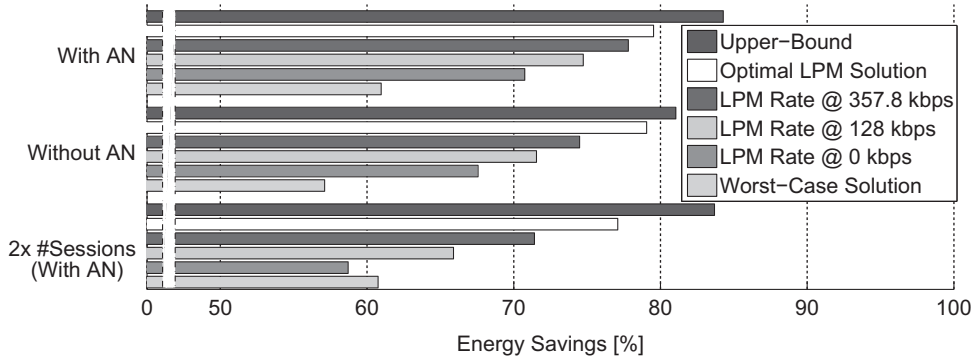


Fig. 7. Average energy savings by single-level LPM in 1000 scenarios compared to full-power mode.

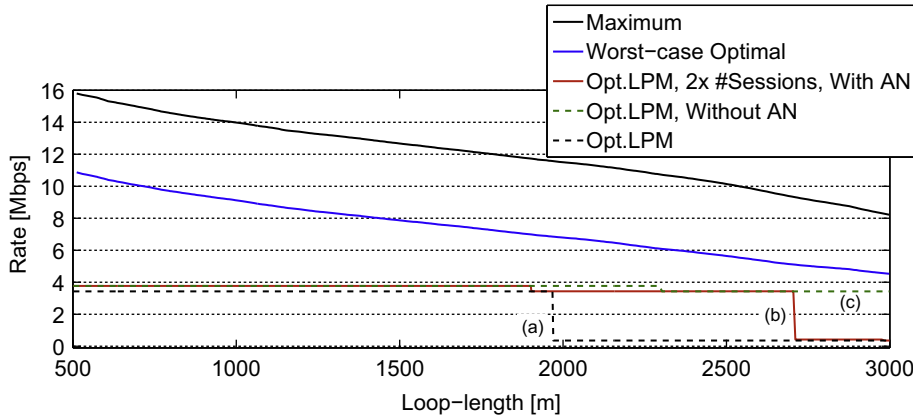


Fig. 8. Dependency of the LPM rate-level under various LPM policies on the loop-length, the noise-level, and the number of sessions.

4.2.1. Optimal LPM rate setting

The results for the achieved average energy savings are presented in Fig. 7 and Table D.1 in Appendix D, beginning with those considering AN as discussed in Section 4.1. Neglecting AN we obtain lower energy savings and a lower objective ratio than in the case with AN, cf. Fig. 7. This is explained by the fact that for short-loop scenarios, differently to the case with AN, the system is rather constrained by the maximum bit-cap constraint (15 bits). This leads to a lower total transmit power and hence LD-power at maximum rate than for long-loop scenarios and therefore to a lower saving potential by LPMs on average. The savings for long loops are however higher without AN than with AN, cf. Section 4.4 for an example. Assuming twice the number $S^{(m)}$ of sessions per day (and AN as above) we obtain a higher average objective, i.e., a higher average sub-optimality of single-level LPM in comparison to continuous rate adaptation, cf. Table D.1 in Appendix D. Intuitively this can be explained by the higher variability of the traffic rate which results from the higher number of sessions. The average link usage over the day is now 30.8% and the average (over scenarios and time) link utilization is as high as 16.1%. This is somewhat comparable to the home access utilization forecast for 2015–2020 in [8] where the predicted link usage and utilization are 30% and 10%, respectively.

In Fig. 8 we compare the LPM rate setting policies in terms of the solutions (rate-levels) depending on the loop length. Empirically we observe that the optimal rates decrease with the loop-length, which seems to be an intuitive consequence of the cost $c(\mathbf{r})$ which increases with the loop-length. Considering the line labelled “(a)” in Fig. 8 as the base-line, we see that a higher number of sessions (cf. the line labelled “(b)”) makes higher LPM rates more efficient as the time one spends in the LPM increases. Neglecting the artificial noise (cf. the line labelled “(c)”) has a similar effect, with the explanation now being the lower cost $c(\mathbf{r})$ which again makes higher LPM rates more efficient.

4.2.2. Fixed LPM rate setting

Next we set the LPM rates independently of the considered traffic and network scenario. Regarding the worst-case LPM setting of Section 2.2 under the standard parameters of Section 4.1 (i.e., including AN) we naturally obtain a lower value for the energy savings than above as the LPM rate-level r is not optimized for the specific traffic at hand, cf. Fig. 7. The same is true for the fixed setting of the LPM rate-level at $r = 128$ kbps and $r = 0$ kbps, respectively.¹³ The

¹³ When $r = 0$ we are not entering LPM unless there is no arrival traffic. The motivation behind a fixed LPM rate at 128 kbps is that voice calls are supposed to be supported during LPM operation.

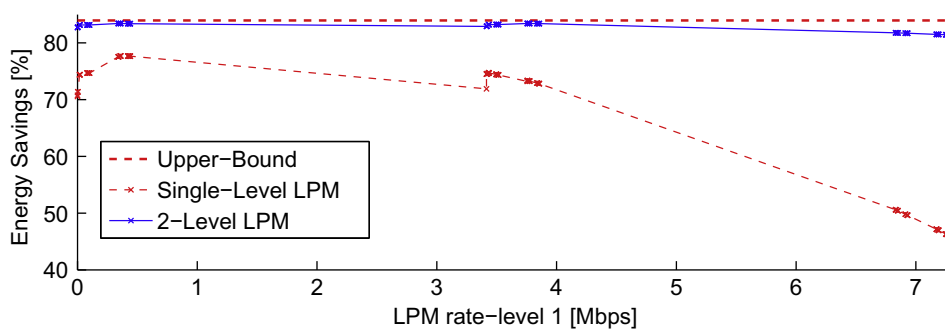


Fig. 9. Dependency of the energy savings compared to the full-power mode on the (lower) LPM rate-level in single and 2-level LPM.

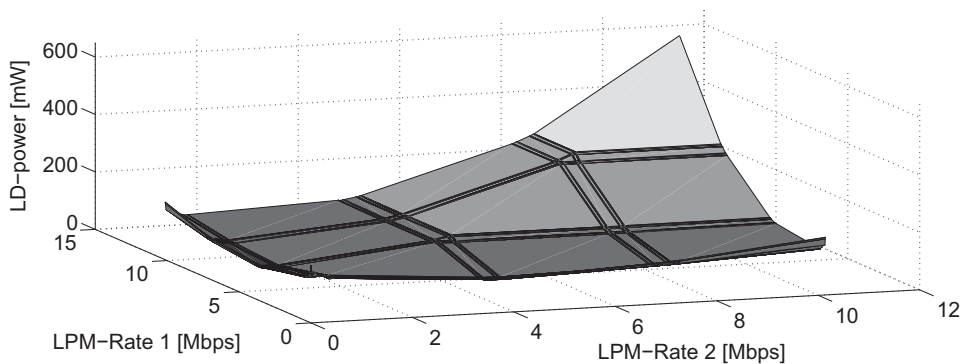


Fig. 10. Performance of 2-level LPMs as a function of the rate setting.

objective ratios in Table D.1 under the optimal worst-case-traffic LPM rate setting in Section 2.2 is even on average close to the theoretical maximum of 2.57 (e.g., 2.48 for the case with AN). When doubling the number of sessions the optimal LPM rate-level increases and the performance of setting the LPM rate to zero drops, cf. Fig. 7. The worst-case rate setting however leads to LPM rates much above the optimal rate-level, and doubling the number of sessions has consequently little impact on the energy-savings, cf. the lowest bar in Fig. 7. Another observation is that a large part of the energy savings (e.g., 74.7% out of the possible 84.3% with AN) can be achieved by simply setting the LPM rate to 128 kbps, especially when the link utilization is low.

4.2.3. A rule of thumb for setting the LPM rate

We observe that the optimal LPM rate under AN (cf. the line labelled “(a)” in Fig. 8) drops at around 2 km to a rate-level of 357.8kbps. This is in fact the sum-rate under the three services video streaming, gaming, and file-sharing, which, besides IPTV, have the largest session durations among the M chosen services, cf. Section 4.1. Considering this selection as a “rule of thumb” we investigate the average performance of this LPM rate selection strategy in Fig. 7. We see that the achieved energy savings are somewhere between those under the optimal LPM rate selection and those under the setting $r = 128$ kbps. Especially when twice the number of sessions are considered we see a substantial

energy saving compared to the other fixed-rate LPM settings as the specific rate-levels of certain applications with long session durations has been taken into account.

As the energy savings by optimal LPM rate selection under AN are similar for different line-lengths (cf. the maximum and minimum savings in Table D.1), and due to the increasing simulation times with an increasing number of LPM and delay states, we proceed by investigating an ADSL2+ scenario with the loop-length fixed at 2500 m.

4.3. Multi-level LPM performance

By increasing the number of LPM rate-levels we expect a lower average power consumption and therefore higher energy savings compared to maximum rate transmission. In Fig. 9 we compare the ideal continuously rate-adapting system’s performance (“Upper-Bound”) to that under (optimally adjusted) single and two-level LPM. While the optimal single-level LPM setting achieves 77.70% of energy-savings, the two-level LPM setting achieves 83.43%, close to the savings achieved by continuous rate adaptation (83.96%). As seen in Fig. 10 the optimal rate-levels for two-level LPM are 0.357 Mbps, which is the optimal rate-level for single-level LPM, and 3.772 Mbps. This example reminds us of the result in Theorem 2, with the important difference that in the simulations we enter LPMs sequentially.

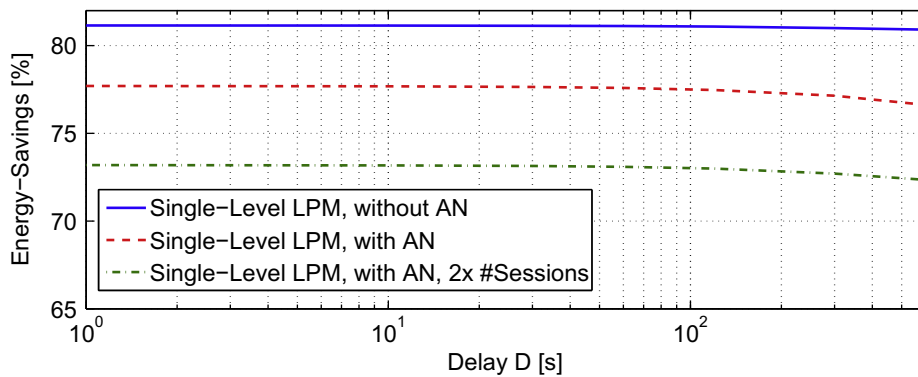


Fig. 11. Delayed LPM performance compared to full-power mode.

Table D.1

Average single-level LPM performance in 1000 ADSL2+ scenarios.

LPM policy	Energy savings [%]			$C^{\pi}(\mathbf{r})/C^{\pi}$		
	Avg.	Min.	Max.	Avg.	Min.	Max.
<i>With AN</i>						
Upper-bound	84.28 ± 0.03	83.52	84.68	1 ± 0.00	1	1
Opt. r	79.53 ± 0.15	77.53	82.83	1.30 ± 0.01	1.12	1.41
Worst-case optimal	60.96 ± 0.01	60.85	61.04	2.48 ± 0.00	2.38	2.54
Fixed-rate, $r = 357.8$ kbps	77.81 ± 0.01	77.53	77.92	1.41 ± 0.00	1.36	1.44
Fixed-rate, $r = 128$ kbps	74.74 ± 0.00	74.61	74.79	1.61 ± 0.00	1.54	1.65
Fixed-rate, $r = 0$ kbps	70.57 ± 0.00	70.56	70.57	1.87 ± 0.00	1.79	1.92
<i>Without AN</i>						
Upper-bound	81.05 ± 0.49	59.86	84.72	1 ± 0.00	1	1
Opt. r	79.06 ± 0.44	59.16	83.43	1.12 ± 0.01	1.02	1.41
Worst-case optimal	57.11 ± 0.51	36.69	61.04	2.35 ± 0.02	1.58	2.55
Fixed-rate, $r = 357.8$ kbps	74.49 ± 0.45	54.98	77.85	1.38 ± 0.01	1.12	1.45
Fixed-rate, $r = 128$ kbps	71.55 ± 0.43	52.79	74.76	1.54 ± 0.01	1.18	1.65
Fixed-rate, $r = 0$ kbps	67.57 ± 0.41	49.85	70.57	1.77 ± 0.02	1.25	1.93
<i>2 × #Sessions (with AN)</i>						
Upper-bound	83.68 ± 0.05	82.06	84.52	1 ± 0.00	1	1
Opt. r	77.09 ± 0.28	71.15	82.04	1.40 ± 0.01	1.16	1.65
Worst-case optimal	60.75 ± 0.03	60.34	61.04	2.41 ± 0.01	2.21	2.52
Fixed-rate, $r = 357.8$ kbps	71.41 ± 0.01	71.15	71.51	1.75 ± 0.01	1.61	1.84
Fixed-rate, $r = 128$ kbps	65.89 ± 0.00	65.78	65.94	2.09 ± 0.01	1.91	2.20
Fixed-rate, $r = 0$ kbps	58.71 ± 0.00	58.71	58.72	2.53 ± 0.01	2.30	2.67

4.4. LPM performance with delay

A delay between state-changes has been proposed as a stabilization method against crosstalk noise fluctuations due to LPMs [2], which can be regarded as an alternative or an add-on to the usage of AN above. This delay can be modeled using additional delay-states as shown in Section 3.3. In Fig. 11 we show the achieved energy-savings by single-level LPM compared to the full-power mode in the exemplary ADSL2+ scenario with a 2500 m long loop. The impact of the delay on the energy-savings for standardized values of D ($D \leq 255$ [1]) can be seen to be fairly small (<1% of the full-power mode LD power consumption), i.e., much less pronounced than the impact of multiple LPMs observed above. The curve simulated without AN seems to be the least influenced by the delay. We note that differently to the average behavior analyzed above, here we obtain a higher saving without AN compared to the

curve simulated with AN, a behavior we attribute to the bit-cap constraint as explained in Section 4.2.

5. Conclusions

An initial calculation of the energy-saving potential by enabling low-power modes (LPMs) in asymmetric digital subscriber lines 2+ (ADSL2+) results in an estimated total energy saving at the central office of 6.7 kWh per year and DSL line, based on an assumed average saving in line-driver (LD) power consumption of 64% of the full power consumption. Our bottom-up approach based on a Markovian traffic and LPM model and a fixed, low LPM rate provides comparable figures (60–75%). The proposed optimization of the LPM rate-level gives additional savings by trading-off the power consumption in the LPM state and the time spent in full-power state, resulting in up to 80%

average savings in LD power. The introduction of multiple LPM levels leads to another 2–7% power savings. Both, the optimization of LPM rate-levels and multiple LPMs were seen to be most effective when the link usage is high (e.g., above 25%) and/or the considered background noise (and hence the rate-cost) is low (e.g., no disturbance from other DSL systems). While we saw that the optimal LPM rate setting depends on various factors, as a rule of thumb the average rates of the low-rate applications with the longest session times (in our case video, file-sharing, and gaming) can be used for an energy-efficient setting of the LPM rate in practice. The studied approach of setting the LPM rates based on worst-case traffic assumptions was seen to be overly conservative under realistic traffic, especially under a low link usage. The introduction of delay between the entrance into LPM states was seen to have little effect on the achieved energy savings, most likely due to the low link usage.

Summarizing, we propose a methodology for the analysis of LPMs with different levels of traffic knowledge, with potential applicability for other communication systems. A single low-power mode under a fixed LPM rate setting accomplishes to save the bulk of the possible energy savings by LPMs in DSL. The optimization of the LPM rates based on the actual traffic statistics bears an additional saving potential which is most visible under a high link usage (e.g., above 25%).

Acknowledgements

The Competence Center FTW Forschungszentrum Telekommunikation Wien GmbH is funded within the program COMET - Competence Centers for Excellent Technologies by BMVIT, BMWA, and the City of Vienna. The COMET program is managed by the FFG.

Appendix A. Proof of Theorem 1

Proof 1. First we recognize that the solution of the maximization in the worst-case LPM problem in (3) is the pdf

$$\pi(\rho) = \begin{cases} 1, & \text{if } \rho = \hat{r}_i, i^* = \operatorname{argmax}_{\{i|1 \leq i \leq L+1\}} \left\{ \frac{c(\hat{r}_{i+1})}{c(\hat{r}_i)} \right\}, \\ 0, & \text{otherwise,} \end{cases} \quad (\text{A.1})$$

where $\hat{\mathbf{r}} \in \mathcal{R}^{L+2}$, $\hat{r}_1 = 0, \hat{r}_2 = r_1, \dots, \hat{r}_{L+1} = r_L, \hat{r}_{L+2} = R$. The objective of setting the LPM rates \mathbf{r} is hence to minimize the maximum ratio in (A.1). As \hat{r}_1 and \hat{r}_{L+2} are fixed this goal is achieved when all ratios in (A.1) are equal, and consequently all ratios equal C^* , that is

$$C^* = \frac{c(\hat{r}_{i+1})}{c(\hat{r}_i)} = \frac{c(\hat{r}_{j+1})}{c(\hat{r}_j)}, \quad \forall i, j, \text{ with } 1 \leq i, j \leq L+1. \quad (\text{A.2})$$

Differently written we have

$$\frac{c(\hat{r}_2)}{c(\hat{r}_1)} \frac{c(\hat{r}_3)}{c(\hat{r}_2)} \dots \frac{c(\hat{r}_{L+2})}{c(\hat{r}_{L+1})} = \frac{c(R)}{c(0)} = (C^*)^{L+1}, \quad (\text{A.3})$$

from where the result on the optimal ratio C^* in (5) follows. Similarly, from (A.2) it follows that $(C^*)^i = c(r_i)/c(0)$ and $(C^*)^{L+1-i} = c(R)/c(r_i)$, which can be written as

$$\sqrt[i]{\frac{c(r_i)}{c(0)}} = \sqrt[L+1-i]{\frac{c(R)}{c(r_i)}}. \quad (\text{A.4})$$

The definition of the optimal LPM levels in (4) follows from (A.4) using the transformation $c_{\text{dB}}(\rho) = 10 \log_{10}(c(\rho))$.

Appendix B. Derivation of lower-bounds for the problem in (6)

In order to derive lower bounds for \tilde{C}^* in (6) we exemplarily pick two types of feasible pdfs $\pi(\cdot)$ in the interval $[0, R]$, namely a uniform distribution $\pi^{\text{uni}}(\rho) = 1/R$ and an exponential distribution $\pi^{\text{exp}}(\rho) = k_1 \exp(-k_2 \rho)$. The pdf $\pi^{\text{exp}}(\rho)$ was chosen for linear cost functions ($d = 1$) in (7) with parameters

$$k_2 = \frac{2c(R) - c(0)}{Rc(R)}, \quad (\text{B.1})$$

$$k_1 = \frac{k_2}{1 - \exp(-k_2 R)}, \quad (\text{B.2})$$

where (B.2) ensures that the pdf integrates to one over the interval $[0, R]$ and (B.1) is a sufficient condition for convexity of the minimization problem in (6). The optimum LPM rate-level r under these settings is now readily obtained by setting the derivative of $C^\pi(r)$ with respect to r to zero, for both, $\pi^{\text{exp}}(\rho)$ under linear costs $\tilde{c}_{(1)}(r)$ as

$$r^* = [r]_0^R, \quad \text{where } \exp(k_2 r) = 1 - \frac{k_2}{k} (kr + c(0) - c(R)), \quad (\text{B.3})$$

where $[\cdot]_0^R$ denotes the projection onto the feasible rate interval $[0, R]$ and k is defined in (7), and for $\pi^{\text{uni}}(\rho)$ under polynomial costs $\tilde{c}_{(d)}(r)$ in (7) as

$$r^* = \frac{R}{\sqrt[d]{d+1}}. \quad (\text{B.4})$$

Appendix C. Proof of Theorem 2

Proof 2. Assume two possible solutions $\mathbf{r}, \tilde{\mathbf{r}} \in \mathcal{R}_+^L$ for $L = 2$ and the optimal solution r^* for $L = 1$ to the problem given in (6) with $r_2 = \tilde{r}_2 \geq r^*$ and $r_1 = r^*, \tilde{r}_1 = r > r^*, \tilde{r}_1 \leq \tilde{r}_2$. The difference in cost as defined in (1) between the two possible solutions is given as

$$\delta = C^\pi(\tilde{\mathbf{r}}) - C^\pi(\mathbf{r}) \quad (\text{C.1a})$$

$$= (c(r) - c(r^*)) \int_0^{r^*} \pi(\rho) d\rho - (c(r_2) - c(r)) \int_{r^*}^r \pi(\rho) d\rho \quad (\text{C.1b})$$

$$\geq (c(r) - c(r^*)) \int_0^{r^*} \pi(\rho) d\rho - (c(R) - c(r)) \int_{r^*}^r \pi(\rho) d\rho \quad (\text{C.1c})$$

$$\geq 0, \quad (\text{C.1d})$$

where (C.1c) holds due to monotonicity of $c(\cdot)$ and $r_2 \leq R$, and (C.1d) holds due to optimality of r^* for our problem in (6) under $L = 1$. In other words, denoting the optimal rates in (6) for $L = 2$ by $\tilde{\mathbf{r}}^*$ we have

$$\tilde{r}_2 \geq r^* \Rightarrow \tilde{r}_1 \leq r^*. \quad (\text{C.2})$$

Conversely assume $r_1 = \tilde{r}_1 \leq r^*$ and $\tilde{r}_2 = r^*$, $r_2 = r < r^*$, $r_2 \geq r_1$, then the difference in cost between the two possible solutions \mathbf{r} and $\tilde{\mathbf{r}}$ is given as

$$\delta = C^\pi(\tilde{\mathbf{r}}) - C^\pi(\mathbf{r}) \quad (\text{C.3a})$$

$$= (c(r^*) - c(r)) \int_{r_1}^r \pi(\rho) d\rho - (c(R) - c(r^*)) \int_r^{r^*} \pi(\rho) d\rho \quad (\text{C.3b})$$

$$\leq (c(r^*) - c(r)) \int_0^r \pi(\rho) d\rho - (c(R) - c(r^*)) \int_r^{r^*} \pi(\rho) d\rho \quad (\text{C.3c})$$

$$\leq 0, \quad (\text{C.3d})$$

where (C.3c) holds again by monotonicity of $c(\cdot)$ and the assumption $r < r^*$, and (C.3d) holds once more by optimality of r^* for our problem in (6) under $L = 1$. This result can be summarized as

$$\tilde{r}_1 \leq r^* \Rightarrow \tilde{r}_2 \geq r^*. \quad (\text{C.4})$$

The result in (8) follows now from (C.2), (C.4), and $\tilde{r}_1 \leq \tilde{r}_2$. \square

Appendix D. Single-level LPM simulation results

See Table D.1.

References

- [1] ITU-T, Asymmetric digital subscriber line transceivers 2 (ADSL2), G.992.3, 2009.
- [2] Network Interoperability Consultative Committee, Guidelines on DSL Power Saving Modes and Non-Stationary Noise in Metallic Access Networks, Tech. Rep. ND1424:2008/02, Version 1.1.1, 2008.
- [3] K. Hooghe, M. Guenach, Toward green copper broadband access networks, IEEE Communications Magazine 49 (8) (2011) 87–93.
- [4] EC Directorate-General JRC Joint Research Centre, Institute for Energy, Renewable Energy Unit, Code of Conduct on Energy Consumption of Broadband Equipment, Version 4, 2011.
- [5] ATIS Exploratory Group on Green, Report on Environmental Sustainability, Tech. Rep., 2009.
- [6] S. Roy, Energy logic: a road map to reducing energy consumption in telecommunications networks, in: International Telecommunications Energy Conference 2008 (INTELEC'08), San Diego, CA, USA, 2008.
- [7] W. Vereecken, W. Van Heddeghem, M. Deruyck, B. Puype, B. Lannoo, W. Joseph, D. Colle, L. Martens, P. Demeester, Power consumption in telecommunication networks: overview and reduction strategies, IEEE Communications Magazine 49 (6) (2011) 62–69.
- [8] R. Bolla, F. Davoli, R. Bruschi, K. Christensen, F. Cucchietti, S. Singh, The potential impact of green technologies in next-generation wireline networks: is there room for energy saving optimization?, IEEE Communications Magazine 49 (8) (2011) 80–86.
- [9] ETSI, Environmental Engineering (EE), The Reduction of Energy Consumption in Telecommunications Equipment and Related Infrastructure, Tech. Rep. ETSI TS 102 530, Version 1.2.1, 2011.
- [10] Sandvine, Global Internet Phenomena Report, Tech. Rep., 2011.
- [11] Press Release of the Bavarian Regulatory Authority for Commercial Broadcasting, 2011. <http://www.blm.de/de/pub/aktuelles/pressemitteilungen.cfm?eventPress=press.DisplayDetail&pressrelease_ID=1644>.
- [12] M. Wolkerstorfer, Energy-Efficient Resource Allocation in Multi-Carrier Digital Subscriber Lines, Ph.D. thesis, Vienna University of Technology, Vienna, Austria, 2012.
- [13] M. Guenach, C. Nuzman, J. Maes, M. Peeters, Y. Li, D. Van Bruyssel, F. Defoort, Power efficient copper access, Bell Labs Technical Journal 15 (2) (2010) 117–129.
- [14] I. Kamitsos, P. Tsiaflikis, S. Ha, M. Chiang, Stable sleeping in DSL broadband access: Feasibility and tradeoffs, in: IEEE Global Communications Conference 2011 (Globecom'11), Houston, Texas, USA, 2011.
- [15] B. Putra, T. Nordström, S. Trautmann, Modeling Energy Efficiency in DSL Systems, Tech. Rep. FTW-TR-2011-001, The Telecommunications Research Center Vienna (FTW), Vienna, Austria, 2011.
- [16] T. Piessens, M. Steyaert, Design and Analysis of High Efficiency Line Drivers for xDSL, Kluwer Academic Publishers, 2004.
- [17] B. Serneels, M. Steyaert, Design of High Voltage xDSL Line Drivers in Standard CMOS, Springer, 2008.
- [18] K. Hooghe, M. Guenach, Towards energy-efficient packet processing in access nodes, in: IEEE Global Communications Conference 2011 (Globecom'11), Houston, Texas, USA, 2011b.
- [19] E. Goma, M. Canini, A. Toledo, N. Laoutaris, D. Kostić, P. Rodriguez, R. Stanojević, P. Valentín, Insomnia in the access or how to curb access network related energy consumption, in: ACM SIGCOMM Computer Communication Review – SIGCOMM '11, vol. 41 (4), Toronto, Canada, 2011, pp. 338–349.
- [20] G. Ginis, Low-Power Modes for ADSL2 and ADSL2+, Tech. Rep., Broadband Communications Group, Texas Instruments, 2005.
- [21] S. Bhaumik, D. Chuck, G. Narlikar, G. Wilfong, Energy-efficient design and optimization of wireline access networks, in: IEEE International Conference on Computer Communications 2011 (INFOCOM'11), Shanghai, China, 2011, pp. 451–455.
- [22] K. Hooghe, M. Guenach, Impact of FITN architecture on access node energy efficiency, in: IEEE Symposium on Communications and Vehicular Technology in the Benelux 2010 (SCVT'10), Enschede, The Netherlands, 2010.
- [23] G. Griffa, L. Radice, C. Bianco, Carbon footprint of next generation fixed networks, in: IEEE International Telecommunications Energy Conference 2010 (INTELEC'10), Orlando, Florida, USA, 2010.
- [24] C. Bianco, F. Cucchietti, G. Griffa, H. Yuping, K. Xiaoming, C. Qiao, L. Shudong, H. Dong, An update on the field trial concerning free cooling solution for FTTCab architecture, in: IEEE International Telecommunications Energy Conference 2009 (INTELEC'09), Incheon, South Korea, 2009.
- [25] C. Bianco, F. Cucchietti, G. Griffa, K. Xiaoming, C. Qiao, H. Yuping, P. Gemma, Z. Liqian, An update on the field trial concerning underground solution for FTTCab architecture, in: IEEE International Telecommunications Energy Conference 2009 (INTELEC'09), Incheon, South Korea, 2009.
- [26] C. Bianco, G. Griffa, N. Lee, P. Gemma, Z. Bin, The energy saving evaluation of Green DSL while in-field mass implementation, in: IEEE International Telecommunications Energy Conference 2011 (INTELEC'11), Amsterdam, The Netherlands, 2011.
- [27] M. Guenach, C. Nuzman, K. Hooghe, J. Maes, M. Peeters, On power-efficient usage of line drivers in copper-based access networks, in: IEEE International Energy Conference and Exhibition (EnergyCon'10), Manama, Bahrain, 2010, pp. 131–136.
- [28] Europe's energy portal, 2011. <www.energy.eu>.
- [29] S. Krumke, Online Optimization – Competitive Analysis and Beyond, Habilitation Treatise, 2001.
- [30] S. Irani, G. Singh, S. Shukla, R. Gupta, An overview of the competitive and adversarial approaches to designing dynamic power management, IEEE Transactions on Very Large Scale Integration (VLSI) Systems 13 (12) (2005) 1349–1361.
- [31] P. Golden, H. Dedieu, K. Jacobsen (Eds.), Fundamentals of DSL Technology, Auerbach Publications, 2006.
- [32] P.E.E. Trojer, Power saving modes for GPON and VDSL2, 2008. <http://www.ieee802.org/3/10GEPON_study/email/pdfV3kikUObAI.pdf>.
- [33] J. Campello, Optimal discrete bit loading for multicarrier modulation systems, in: IEEE International Symposium on Information Theory 1998 (ISIT'98), Cambridge, MA, USA, 1998, p. 193.
- [34] ITU-T, Asymmetric digital subscriber line transceivers (ADSL) – extended bandwidth ADSL2 (ADSL2+), G.992.5, 2005.
- [35] D.P. Bertsekas, Nonlinear Programming, Athena Scientific, 1999.
- [36] M. Needham, J. Harris, Traffic and network modeling for next generation applications, in: IEEE International Symposium on Broadband Multimedia Systems and Broadcasting, Las Vegas, Nevada, USA, 2008.

- [37] J. Cosmas, J. Loo, A. Aggoun, E. Tsekleves, Matlab traffic and network flow model for planning impact of 3D applications on networks, in: IEEE International Symposium on Broadband Multimedia Systems and Broadcasting, Shanghai, China, 2010.
- [38] D. Levin, Y. Peres, E. Wilmer, Markov Chains and Mixing Times, American Mathematical Society, 2008.
- [39] B. Philippe, Y. Saad, W. Stewart, Numerical methods in Markov chain modeling, *Operations Research* 40 (6) (1992) 1156–1179.
- [40] ETSI, Transmission and Multiplexing (TM); Access Transmission Systems on Metallic Access Cables; Very High Speed Digital Subscriber Line (VDSL); Part 1: Functional Requirements, TM6 TS 101 270-1, Version 1.3.1, 2003.



Martin Wolkerstorfer received the “Dipl. Ing.” degree (equivalent to a master's degree) in electrical engineering from Graz University of Technology, Austria, in 2007, and the Ph.D. degree from Vienna University of Technology, Austria, in 2012, respectively. He is currently working as a senior researcher in the field of signal and information processing at the FTW Telecommunications Research Center Vienna, Austria. His research interests include the application of optimization theory in communications and signal processing, and

energy-efficient broadband access networks.



Driton Statovci received the “Inxh. Dipl.” degree (equivalent to a master's degree) in 1996 from University of Prishtina, Kosova. He received the Ph.D. degree in 2005 from Vienna University of Technology, Austria. Currently he is with the FTW Telecommunications Research Center Vienna, Austria, working as a senior researcher and project manager. Since 2006 he is working as a guest lecturer at the University of Prishtina, Kosova. His current research interests include multi-user transmission theory, multi-carrier modulation,

interference mitigation and cancelation, the application of convex and non-convex optimization techniques in communication systems, and energy-efficient system design and operation.



Tomas Nordström received the M.S.E.E. degree in 1988, the licentiate degree in 1991, and the Ph.D. degree in 1995, all from Luleå University of Technology, Sweden. Between 1996 and 1999, he was with Telia Research (the research branch of the Swedish incumbent telephone operator) where he developed broadband Internet communication over twisted copper pairs. In December 1999 he joined the FTW Telecommunications Research Center Vienna, Austria, where he currently works as a Key Researcher in the field of

“Broadband wireline access”. During his years at FTW he has worked on various aspects of wireline communications like simulation of xDSL systems, cable characterization, RFI suppression, exploiting the common-mode signal in xDSL, and more recently dynamic spectrum management. Since 2009 he is also holding a position as an Associate Professor in Computer Systems Engineering at Halmstad University (HH), Sweden. His current research interests include all aspects of energy efficient computer and communication systems, from cross-layer design and signal processing all the way to novel power amplifier designs and multi-core computing.